Chemical Research in Toxicology

pubs.acs.org/crt

Article

Metabolic Activation of 2-Methylfuran to Acetylacrolein and Its Reactivity toward Cellular Proteins

Verena Schäfer, Simone Stegmüller, Hanna Becker, and Elke Richling*

Cite This: https://doi.org/10.1021/acs.chemrestox.4c00083

Read Online

ACCESS | Metrics & More | Article Recommendations | Supporting Information

ABSTRACT: 2-Methylfuran (2-MF) is a process-related contaminant found primarily in heat-treated foods, such as coffee or canned food. The oxidative metabolic activation of 2-MF is supposed to follow the pathway established for furan, which is known to generate the highly reactive metabolite butenedial (BDA). In the case of 2-MF, generation of the BDA homologue 3-acetylacrolein (AcA) is to be expected. 2-MF metabolism to AcA was investigated in two model systems: commercial microsomal preparations and primary rat hepatocytes (pRH). To scavenge the generated 2-MF, two model nucleophils, *N*-acetyl-L-cysteine (AcCys) and *N*-α-acetyl-L-lysine (AcLys), were used, and the formation of the corresponding adducts was measured in the supernatants. The metabolic activation of 2-MF to AcA was studied using human liver microsomes as well as rat liver microsomes. Incubation of 2-MF in Supersomes allowed to identify the cytochrome P450 isoenzyme primarily responsible for 2-MF. In addition, primary rat hepatocytes were incubated with 2-MF or AcA and AcLys adduct of AcA (*N*-α-acetyl-L-lysine-acetylacrolein, AcLys-AcA) determined in the cell supernatants by UHPLC-MS/MS. In model experiments, AcA formed adducts with AcCys and AcLys. The structures of both adducts were characterized. For incubations in biological activating systems, CYP 2E1 was found to be a key enzyme for the conversion of 2-MF to AcA in Supersomes. When pRH were incubated with 2-MF and AcA, AcLys-AcA was detected in the cell supernatants in a time- and dose-dependent manner. The results showed that AcA was indeed formed at the cellular level. In contrast to the AcLys-AcA adduct, no *N*-acetyl-L-cysteine-acetylacrolein (AcCys-AcA) adduct could be detected in pRH. AcA was determined as a reactive metabolite of 2-MF *in vitro*, and its adduct formation with nucleophilic cellular components was evaluated. The metabolites were characterized, and AcLys-AcA was identified as potential biomarker.

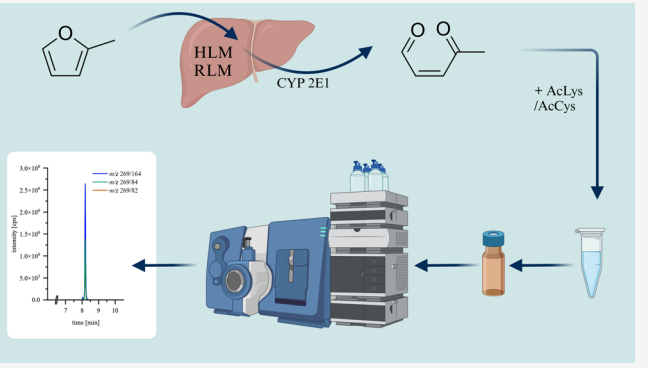

INTRODUCTION

2-Methylfuran (2-MF) can be found as a heat-induced contaminant in foods, sometimes at high levels. In particular, it can be formed by heat treatment from ubiquitous precursors such as amino acids and carbohydrates but also fatty acids. However, as the European Food Safety Authorities (EFSA) panel on Contaminants in the Food Chain (CONTAM) stated data for risk assessment is not only incomplete in terms of exposure but also in terms of toxicity.[1] The main source of exposure for adults is coffee with an average content of 1328 μg/kg up to a maximum value of 8680 μg/kg.[2,3] Rahn and Yeretzian reported amounts of 99.05 μg/l furan and 263.91 μg/l 2-MF in coffee brews prepared by automatic machines.[4] Infants are exposed by cereal products, such as cereals (23.5 μg/kg) or porridge in jars (68.3 μg/kg).[1,5] Recently, flakes and cornflakes, extruded cereals, puffed grains, and granolas were analyzed for their furan and alkylfuran contents. Highest amounts were found for furan and 2-pentylfuran. Concerning 2-MF 6.55 μg/kg was found in commercially available muesli and granola, 52.8 μg/kg in puffed grains, and highest observed 2-MF levels in puffed barley and puffed oat from 6.4 to 252 μg/kg (mean 52.8 μg/kg), but still lower than furan levels, respectively.[6]

In vivo tests in rats showed liver-damaging effects of 2-MF, about comparable to the effects of the better-studied contaminant furan for which induction of cholangiofibrosis was observed in long-term rodent studies.[7] Furan was classified by the International Agency for Research on Cancer (IARC) as "possibly carcinogenic to humans" (class 2B). The toxicity of furan is based on metabolic activation to the reactive intermediate *cis*-2-butene-1,4-dial (BDA), which can react with nucleophilic cell components. While the formation of protein adducts has already been demonstrated *in vivo*, some indications for DNA adducts have been reported after furan

Received: February 28, 2024
Revised: July 12, 2024
Accepted: July 19, 2024

exposure, but these could not be unequivocally characterized. Mutagenic properties were observed in the Ames test. Therefore, the question of the mode of action (MOA) arises for the risk assessment; i.e., the question of whether furan is a genotoxic carcinogen or whether it acts by an indirect mechanism is unresolved up to present.[1]

For 2-MF, an analogue cytochrome P450 (CYP)-mediated metabolic activation via oxidative ring opening to 3-acetylacrolein (AcA, 2-oxopent-2-enal) was assumed. Metabolic activation of 2-MF to the putative reactive intermediate AcA, showing high binding reactivity to amino acids, was proposed.[8,9] As an α,β-unsaturated carbonyl compound, AcA has the potential to react with nucleophilic centers in proteins and DNA. Michael addition to the double bond or nucleophilic addition to the aldehyde or keto group has been postulated.[8] Distribution and binding studies with ^{14}C-labeled 2-MF showed binding to proteins and DNA *in vitro* and *in vivo*. The highest levels of radio-labeled substance were detected in liver, followed by lung, kidney, and blood.[10] Subacute *in vivo* studies in rats confirmed the liver as the main toxicological target of 2-MF. Necrosis and fibrosis were also found to a lesser extent in the lungs.[11] However, there is a lack of data concerning long-term exposure to 2-MF.

The CONTAM Panel of EFSA has used the total exposure to furan, 2-MF, and 3-methylfuran (3-MF) for a preliminary risk assessment. When considering the amounts in the diet of adults, the Margin of Exposure (MoE) was below 100 in 50% of the estimations. The induction of cholangiofibrosis by furan was used as a specific end point for the calculation.[12] In addition, 2-MF accounts for a significant proportion of the total exposure of summarized furans, with some foods contributing considerably higher exposure to 2-MF than to furan. According to the EFSA's CONTAM Panel, there is an urgent need for research on occurrence and factors of influence of 2-MF formation. Moreover, long-term effects, such as carcinogenicity, need to be investigated *in vivo*. Finally, for risk characterization it is mandatory to elucidate molecular and cellular mechanisms underlying toxicological effects.[1]

We report here the generation of AcA as a reactive metabolite of 2-MF *in vitro* and its adduct formation with nucleophilic cellular components in the chemical model experiments using Supersomes and microsomes as well as by the use of primary rat hepatocytes (pRH).

MATERIALS AND METHODS

For use in synthesis, 2,5-dihydro-2,5-dimethoxy-2-methylfuran (97%, mixture of *cis* and *trans*, DHDMMF), *N*-α-acetyl-L-lysine (AcLys), and *N*-α-acetyl-L-cysteine (AcCys) were purchased from Sigma-Aldrich (St. Louis, USA), whereas acetic acid (99%) was from Avantor Performance Materials B.V. (Radnor, USA). For preparative purposes, HPLC-grade formic acid and acetonitrile were purchased from Sigma-Aldrich (St. Louis, USA) and Fisher (Schwerte, Germany), respectively, whereas MS-grade solvents formic acid and acetonitrile were purchased from Carl Roth (Karlsruhe, Germany) and Merck (Darmstadt, Germany), respectively. All other solvents and chemicals were of p.a. grade. NMR and MS spectra of the adducts, as well as the structural assignment of their signals, are included in the Supporting Information.

Synthesis. *L-2-Acetamido-6-(2-methyl-5-oxo-2,5-dihydro-1H-pyrrol-1-yl)hexanoic Acid (AcLys-AcA).* The method of acid hydrolysis was modified according to Chen et al. (1997).[13] Briefly, 2,5-dihydro-2,5-dimethoxy-2-methylfuran (39.5 μL; 273 μmol; DHDMMF) was stirred in 0.1% aqueous acetic acid (1.961 mL) for 1 h at 37 °C (500 rpm) before adding *N*-α-acetyl-L-lysine (AcLys) (51.39 mg; 273 μmol) dissolved in 2 mL of water. The solution was stirred for 24 h at 37 °C and a further 10 h after addition of 6.13 μL acetic acid (100%). Purification of the desired AcLys-AcA adduct was performed in two runs by semipreparative HPLC using an Agilent 1200 series HPLC system (Waldbronn, Germany) equipped with a Synergi 4 μm Polar-RP column (250 × 10 mm, Phenomenex, Torrance, USA). For the first run, the synthesis mixture was diluted 1:2 with H_2O_{dd} and injected in aliquots of 2 mL using a mobile phase of 0.1% aqueous formic acid (A) and acetonitrile (B) at a flow rate of 8 mL/min. The gradient started at 5% B, was kept isocratic for 2 min, and the percentage of B was increased to 20% over 13 min, then to 50% B over 0.5 min and remained for 2.5 min. Afterward, the HPLC column was rinsed with 5% B for 4 min to prepare for the next cycle, which was started after at least 5.0 min of equilibration under the initial solvent conditions. Fractions of 0.5 min were collected and analyzed by HPLC-ESI-MS/MS (HPLC 1200 series, Agilent, coupled to a Sciex MS API 3200 instrument (Applied Biosystems, Darmstadt, Germany)). Pooled fractions were purified again by the HPLC method described above. In the first run, the desired product AcLys-AcA eluted between 5.0 and 7.5 min, and in the second run, it eluted between 6.0 and 8.0 min. Their volumes were reduced to ~10 mL under reduced pressure (20 mbar; 1400 rpm; 30 °C), and the residue was lyophilized (0.47 mbar; 15 °C). The yield was 29.067 mg (108.3 μmol; 40%; white solid). Purity was not determined (^{1}H NMR), but no other signals were observed.

AcLys-AcA (268.31 g/mol, $C_{13}H_{20}N_2O_4$). **^{1}H NMR (600 MHz, D_2O).** δ [ppm] 4.29 (dd, J = 8.7, 4.8, 1H), 3.26−3.17 (m, 2H), 3.15 (t, J = 6.7 Hz, < 1H), 2.83 (t, J = 6.6 Hz, <1H), 2.56−2.48 (m, 1H), 2.45−2.36 (m, 1H), 2.26−2.20 (m, 1H), 2.19 (s, <1H), 2.12−2.04 (m, 1H), 2.01 (s, 3H), 1.91−1.81 (m, 1H), 1.78−1.69 (m, 1H), 1.63−1.54 (m, 2H), 1.50 (d, J = 10.0 Hz, 2H), 1.44−1.31 (m, 2H). Spectrum and structural assignments are shown in Supporting Information Figure S1 and Table S1.

^{13}C NMR (101 MHz, D_2O). δ [ppm] 177.53, 176.07, 174.97 (low intensity (0.5−0.05)), 174.21, 91.18 (d, J = 3.9 Hz), 52.76 (d, J = 5.6 Hz), 38.85, 38.70 (d, J = 2.5 Hz), 30.03 (d, J = 2.3 Hz), 29.28, 28.59 (d, J = 8.8 Hz), 27.76 (d, J = 8.1 Hz), 22.59 (d, J = 1.5 Hz), 22.23, 21.48.

^{1}H NMR (600 MHz, MeCN-d_3). δ [ppm] 7.02−6.93 (m, 0.48H), 6.89 (d, J = 8.6 Hz, 0.23H), 6.80 (d, J = 8.3 Hz, 0.22H), 4.17 (s, 0.35H), 4.16−4.11 (m, 1H), 4.05 (s, 0.31H), 3.42−3.29 (m, 0.61H), 3.22−2.97 (m, 1.39H), 2.66−2.55 (m, 1H), 2.44−2.13 (m, 3H), 2.03 (s, 1,22H), 1.86−1.83 (m, 3H), 1.76−1.54 (m, 2H), 1.55−1.38 (m, 2H), 1.35 (d, J = 3.1 Hz, 2H), 1.31−1.22 (m, 2.15H).

^{13}C NMR (151 MHz, MeCN-d_3). δ [ppm] 208.62, 177.03, 175.47, 173.97, 171.67, 148.16, 142.36, 90.92, 83.99, 53.29 (d, J = 20.7 Hz), 39.72, 39.21, 38.92, 37.27, 35.54, 35.47, 30.28, 29.91, 29.66, 29.51, 26.71, 26.49, 24.34, 23.57, 23.41, 23.30, 22.59, 13.66.

^{1}H NMR (400 MHz, DMSO-d_6). δ [ppm] 12.32 (s), 7.96 (d, J = 7.1 Hz, 1H), 5.60 (s), 4.14 (q, J = 7.7 Hz, 1H), 3.04 (m, 2H), 2.62 (t, J = 6.9 Hz, 0.4H), 2.41−2.24 (m, 1.2H), 2.21−2.10 (m, 0.7H), 2.08 (s, 0.4H), 2.04−1.88 (m, 1.4H), 1.85 (s, 3H), 1.75−1.63 (m, 1H), 1.62−1.41 (m, 3H), 1.36 (s, 2.6H), 1.30 (m, 2H).

^{13}C NMR (151 MHz, DMSO). δ [ppm] 207.51, 176.92, 175.20, 173.87, 173.32, 170.98, 169.35, 146.71, 141.06, 98.73, 88.90, 83.47, 51.84, 51.71, 38.80, 38.29, 38.06, 37.94, 37.94, 36.19, 34.48, 30.74, 30.74, 29.71, 29.11, 28.81, 28.69, 28.38, 26.62, 25.64, 23.35, 23.23, 22.91, 22.85, 22.36, 13.24.

HPLC-ESI$^+$-MS/MS. MS^2 [m/z] 269.15/251.14 [M-O]$^+$; 227.14 [M-$COCH_3$]$^+$; 223.14 [M-COOH]$^+$; 181.13 [M-$COCH_3$−COOH]$^+$; 164.11 [M-$COCH_3$−COOH-NH]$^+$; 132.10 [M-(pyrrolin-2-on)]$^+$; 126.09 [M-(pyrrolin-2-on)-COOH]$^+$; 98.06; 84.06 [M-(AcLys-N)-O]$^+$; 82.07. The MS^2-spectrum is shown in Supporting Information Figure S2.

UV/Vis (H_2O): λ_{max} = 250 nm.

2-Acetamido-3-((5-methylfuran-3-yl)thio)-propionic Acid (AcCys-AcA). The synthesis of AcCys-AcA was performed after Chen et al. (1997)[13] with modifications. 2,5-Dihydro-2,5-dimethoxy-2-methylfuran (14.16 μL; 100 μmol; DHDMMF) was stirred in 0.1% aqueous acetic acid (986 μL) for 1 h at 37 °C (500 rpm) before adding *N*-α-acetyl-L-cysteine (8.160 mg; 50 μmol) dissolved in 1 mL

https://doi.org/10.1021/acs.chemrestox.4c00083
Chem. Res. Toxicol. XXXX, XXX, XXX−XXX

of water. The solution was stirred for 24 h at 37 °C and a further 10 h after addition of 5 μL of acetic acid (100%). The reaction mixture was separated semipreparatively (previous section) in two steps, whereby the fractions checked by mass spectrometry were combined. Their volumes were reduced to ∼10 mL under reduced pressure (20 mbar; 1400 rpm; 30 °C), and the residue was lyophilized (0.47 mbar; 15 °C). The yield was 4.356 mg (17.9 μmol, 36%; white solid) with a purity (^{1}H NMR) of 97%.

AcCys-AcA (243.06 g/mol, C10H13NO4S). **^{1}H NMR (600 MHz, D_2O):** δ [ppm] 6.54 (d, *J* = 3.1 Hz, 1H), 6.09 (m, 1H), 4.48 (dd, *J* = 8.2, 4.1 Hz, 1H), 3.25 (dd, *J* = 14.3, 4.1 Hz, 1H), 3.07 (dd, *J* = 14.3, 8.3 Hz, 1H), 2.27 (s, 3H), 2.00 (s, 3H). The spectrum and structural assignments are shown in Supporting Information Figure S3 and Table S2.

AcCys-AcA (243.06 g/mol, $C_{10}H_{13}NO_4S$). **^{1}H NMR (600 MHz, DMSO-d_6).** δ (ppm) 8.26 (d, *J* = 7.9 Hz, 1H), 6.53 (d, *J* = 2.8 Hz, 1H), 6.13 (m, 1H), 4.30 (td, *J* = 8.4, 4.7 Hz, 1H), 3.08 (dd, *J* = 13.6, 4.6 Hz, 1H), 2.89 (dd, *J* = 13.4, 8.8 Hz, 1H), 2.27 (s, 3H), 1.85 (s, 3H).

^{13}C NMR (151 MHz, D_2O). δ [ppm] 173.99, 173.86, 156.81, 140.46, 120.10, 107.91, 53.07, 36.17, 21.60, 12.92.

HPLC-ESI$^-$-MS/MS: MS^2 [*m*/*z*] 241.9/113.0 [M-(AcCys-S)]$^-$; 85.0 [M-(MF-S)-H_2O]$^-$; 70.0 [M-(MF-S)-H_2O−CO_2]$^-$. The MS^2 spectrum is shown in Supporting Information Figure S4.

UV/Vis (H_2O): λ_{max} = 250 nm; 223 nm.

HPLC-ESI-MS/MS identification of the synthesis product AcCys-AcA (and later used for metabolism in pRH) was as follows: An HPLC-MS/MS system of AB Sciex was used. The quantification was performed using an Agilent Technologies Binary SL 1200 liquid chromatography system (Waldbronn, Germany), consisting of a binary pump (G1312A), an autosampler (G1367C) with thermostat, and a variable-wavelength detector (G1315C) coupled to a SCIEX API 3200 triple quadrupole mass spectrometer (Applied Biosystems, Darmstadt, Germany). The latter was equipped with an electrospray ionization source (ESI), operating in the multiple reaction mode (MRM) with negative electrospray ionization (ESI$^-$). The ESI-MS conditions were as follows: ion spray voltage (IS) −4500 V; curtain gas (CUR) 50 psi; nebulizer gas 35 psi; heater gas 50 psi; temperature (*T*) 550 °C; declustering potential (DP) −40 V for AcCys-AcA; focusing potential (FP) 340 V; entrance potential (EP) −10.5 V; collision cell entrance potential (CEP) −16 V. HPLC conditions were as follows: Synergi Hydro-RP 4 μm polar RP 80 Å column (150 mm × 3 mm, Phenomenex, Torrance, California, USA) and a Synergi Aqua C18 guard column (4 μm); solvent system: A 0.1% formic acid, B acetonitrile; gradient profile: isocratic 5% B for 5 min, within 0.1 min from 5 to 25% B and over 7 min to 67% B and within 0.05 min to 95% B, isocratic for 3 min, from 95 to 1% B over 0.05 min and isocratic 1% B for 1.5 min; flow rate 600 μL/min; injection volume 10 μL; column oven temperature 25 °C. For the calibration of AcCys-AcA, a concentration series of 0.001−50 μM was prepared in the starting composition of the superplasticizer (5% MeCN; 95% water with 0.1% formic acid). Samples were membrane-filtered (0.45 μm) prior to injection; Retention time was 9.0 min. ESI$^-$-MS/MS in the MRM method in positive mode was used to detect AcCys-AcA with the mass transition *m*/*z* 241.9/112.9 as a quantifier, after which *m*/*z* 241.9/69.9 and *m*/*z* 241.9/84.9 were used as qualifiers.

The precision of the method 2.5 to 1000 nM AcCys-AcA was determined by intra- (five replicate analysis of one concentration of AcCys-AcA in a row) and interday (one concentration of AcCys-AcA on 5 days in a row) repetition experiments; the coefficient of variation was 3.2% for intraday and 3.4% for interday experiments. LOD was determined as 1 nM (calculated) and LOQ as 2.5 nM using a calibration approach adapted from the European Commission/Joint Research Centre Guidance Document (2023).[14]

L-2-Acetamido-6-(2-oxo-2,5-dihydro-1H-pyrrol-1-yl)hexanoic Acid (AcLys-BDA). The method of acid hydrolysis was modified according to Chen et al. (1997).[13] Briefly, 2,5-dihydro-2,5-dimethoxyfuran (33.2 μL; 273 μmol; DHDMFu) was stirred in 0.1% aqueous acetic acid (1.961 mL) for 1 h at 37 °C (500 rpm) before adding *N*-α-acetyl-L-lysine (51.39 mg; 273 μmol) dissolved in 2 mL of water. The solution was stirred for 24 h at 37 °C and a further 10 h after addition of 6.13 μL of acetic acid (100%). Purification of the desired AcLys-BDA adduct was performed in two runs by semipreparative HPLC using an Agilent 1200 series HPLC system (Waldbronn, Germany) equipped with a Synergi 4 μm Polar-RP column (250 × 10 mm, Phenomenex, Torrance, USA). Details see above. Fractions of 0.5 min were collected and analyzed by HPLC-ESI-MS/MS (HPLC 1200 series, Agilent, coupled to a Sciex MS API 3200 (Applied Biosystems, Darmstadt, Germany)). Pooled fractions were purified again by the HPLC method described above. In the first run, the desired product AcLys-BDA eluted between 7.0 and 8.5 min and in the second run between 8.0 and 12.0 min. Their volumes were reduced to ∼10 mL under reduced pressure (20 mbar; 1400 rpm; 30 °C), and the residue was lyophilized (0.47 mbar; 15 °C). The yield was 11.097 mg (43.6 μmol, 16%, white solid). Purity 96% (^{1}H NMR).

AcLys-BDA (254.28 g/mol, $C_{12}H_{18}N_2O_4$). **^{1}H NMR (600 MHz, DMSO-d_6).** δ [ppm] 8.12 (d, *J* = 7.7 Hz, 1H), 7.31 (d, *J* = 5.9 Hz, 1H), 6.12 (d, *J* = 5.9 Hz, 1H), 4.16 (dq, *J* = 8.3, 5.3 Hz, 1H), 4.05 (s, 2H), 3.35 (td, *J* = 7.1, 2.9 Hz, 2H), 1.87 (s, 3H), 1.76−1.68 (m, 1H), 1.64−1.57 (m, 1H), 1.57−1.46 (m, 2H), 1.28 (p, *J* = 7.3, 6.8 Hz, 3H). Spectrum and structural assignments are shown in Supporting Information Figure S5 and Table S3.

^{13}C NMR (151 MHz, DMSO). δ (ppm): 173.85, 170.50, 169.36, 144.58, 126.87, 52.34, 51.71, 40.84, 30.63, 27.66, 22.67, 22.35.

HPLC-ESI$^+$-MS/MS. MS^2 [*m*/*z*] 255.13/237.12 [M-O]$^+$; 213.12 [M-$COCH_3$]$^+$; 209.13 [M-COOH]$^+$; 167.12 [M-$COCH_3$−COOH]$^+$; 150.09 [M-$COCH_3$−COOH-NH]$^+$; 132.10 [M-(pyrrolin-2-on)]$^+$; 126.09 [M-(pyrrolin-2-on)-COOH]$^+$; 124.08; 84.04 [M-(AcLys-N)]$^+$. The MS^2-spectrum is shown in Supporting Information Figure S6.

UV/Vis (H_2O): max = 254 nm.

Incubations with Microsomes and Supersomes. Microsomes of rats (RLM, Corning Genetest Rar Sprague−Dawley, pooled liver microsomes, male ref.452501) and humans (HLM 150, Corning UltraPool human liver microsomes, mixed gender, ref.452117) were purchased from Corning (Glendale, USA). Supersomes (supersomes human and CYP 1A2, 3A4, 2A6, 2C9, 2D6, and 2E1) were also purchased at Corning, Glendale, USA. All solutions used are summarized in Table S4 and Table S5. The protocol was as follows: After the microsomes or Supersomes were fast defrosted at 37 °C and 300 rpm, preincubations were gently shaken in an incubator (TH-30; Carl Roth, Karlsruhe, Germany) at 37 °C for 5 min. They constrained the substrate, microsome or Supersome, 50 mM K_2HPO_4 or tris buffer (depending on CYP), 3 mM $MgCl{\cdot}6H_2O$ and 4 mM AcLys. After preincubation with substrate for 5 min at 37 °C (300 rpm), the reactions were started by addition of NADPH. Incubations with Supersomes (CYP 1A2, 3A4, 2A6, 2C9, 2D6, and 2E1, 120 nM) were performed with 100 or 500 μM 2-MF for 10, 30, and 60 min. Liver microsomes (1.0 mg of microsomal protein/mL) or Supersomes (CYP 2E1, 120 nM) were at first incubated with varying times of 1, 5, 10, 15, 30, 60, and 120 min with 100 and 500 μM 2-MF. Incubations with different substrate concentrations from 10, 100, 250, 500, and 750 μM 2-MF for 10 min followed. Control incubations were carried out with heat-inactivated microsomes or Supersomes (inactivation: 30 min, 90 °C, 600 rpm) with 100 and 500 μM 2-MF at 37 °C and with intact microsomes/Supersomes but without NADPH. The reaction was stopped with ice-cold MeCN (100%, −20 °C) containing internal standard (IS) AcLys-BDA (1 μM). After centrifugation (4 °C, 17,000*g*) for 10 min, the supernatant was membrane-filtered, acidified (2 μL 25% formic acid), and AcLys-AcA analyzed by HPLC-MS/MS. All incubations were performed at least three times (n = 3−6) in independent experiments.

The recovery of 10, 800, 1000, and 1200 nM AcLys-AcA in the sample matrix after treatment was 101 ± 3%.

Incubations of 2-MF and AcA with pRH. Primary rat hepatocytes (pRH) were isolated from livers of adult male Wistar rats (150−250 g bw) anaestesized with pentobarbital (100 mg/kg bw; i.p.) according to the procedure described by Schrenk et al. (1992)[15] with minor modifications (in accordance with legal regulations in 2019). Freshly isolated hepatocytes were obtained by in situ liver

https://doi.org/10.1021/acs.chemrestox.4c00083
Chem. Res. Toxicol. XXXX, XXX, XXX−XXX

perfusion: Livers were perfused with EGTA (3,12-Bis-(carboxymethyl)-6,9-dioxa-3,12-diazatetradecane-1,14-dioic acid) buffer, followed by perfusion with a collagenase buffer. Cell count and viability were determined using a Neubauer counting chamber after dilution with Trypan blue (0.1%).

Cytotoxicity was determined via cell viability using resazurin reduction.[16] Only cell suspensions with a viability ≥80% were used. The seeding of the cells was dependent on the subsequent experiment, but prior growth in the required cell number in the corresponding cultivation vessel was necessary. After 3 h in fresh culture medium (37 °C, 5% CO_2, 95% humidity), the medium with dead cells was removed. The cells were used directly for investigations, as their viability began to decline after 48−72 h and were no longer suitable for metabolic studies. In pRH cytotoxicity was determined at 1, 6, 18, 24, or 48 h and concentrations of 10, 50, 100, 500, and 1000 μM 2-MF or 0.1, 0.5, 1, and 5 μM AcA.

In vitro studies were performed as follows: To allow the pRH to grow, the cell culture dishes to be used (100 mm) had to be evenly moistened with collagen solution (0.5 g of collagen/1 L of 0.1% acetic acid) and dried overnight. The freshly isolated pRH were diluted with culture medium to 1 million cells/mL, and 7 mL of cell suspension was seeded per collagenized 100 mm dish. After the cells had grown for 3 h, they were washed with PBS, and incubation was started in an incubator (37 °C, 5% CO_2, 95% humidity) with the addition of 7 mL of incubation solution/cell culture dish (100 mm). For each test concentration, two cell culture dishes (100 mm) were prepared per sample in order to guarantee a sufficient yield of cell supernatant. At the end of the incubation period of 1, 6, 18, 24, or 48 h, the cell supernatant was transferred to 15 mL centrifuge tubes and the cells were washed with PBS. The samples were kept on ice and then stored at −80 °C until further processing via SPE and UHPLC-MS/MS measurements. Dose response experiments were performed using 2-MF concentrations of 10, 50, 100, 500, and 1000 μM or 0.1, 0.5, 1, and 5 μM AcA (synthesis see Schäfer et al. 2024[17]). After incubation, the cell culture medium was analyzed after enrichment via SPE and purification via UHPLC-ESI-MS/MS.

AcLys-BDA was used as an internal standard with a final concentration of 1 μM for the samples to be measured. For preparation, the SPE column (Chromabond HR-XA column; 200 mg, 3 mL, Macherey-Nagel) was conditioned with 3 mL of MeCN and 3 mL of ammonium formate buffer (100 mM) was equilibrated. The sample preparation consisting of 4−8 mL cell supernatant, 4−8 mL ammonium formate buffer, and 10 μL IS (100 μM) was applied to the column and then washed with 3 mL ammonium formate buffer. The test substances were eluted by adding 5 mL of elution buffer (100 mL of ammonium formate buffer). The rinsing step with 3 mL of MeCN was not collected. The eluate was concentrated in a vacuum centrifuge (20 mbar, 1400 rpm, RT), acidified with 50 μL formic acid (100%), made up to 1 mL H_2O and transferred to a 1.5 mL vial. The amount of AcLys-AcA in pRH was determined with the method described below (UHPLC-ESI^+-MS/MS; API 5500) (n = 3−6 independent experiments).

Analyte concentrations of 10, 40, 50, and 60 nM were selected to determine the recovery of AcLys-AcA in cell supernatants after processing using SPE. They reflect the average concentrations to be expected (80%, 100%, 120%), known from the preliminary tests, as well as the limiting observation. The recovery rate was 81.2 ± 3.9%.

Additionally, the DNA of pRH was isolated and analyzed using stable isotope dilution analysis (SIDA) and HPLC-ESI-MS/MS techniques and will be reported in Schäfer et al. 2024.[17]

Quantification of AcLys-AcA in Incubations with Microsomes. Quantification of AcLys-AcA in the microsomal and Supersomes incubations was performed with AcLys-BDA as an internal standard. The quantification was performed using an Agilent Technologies Binary SL 1200 liquid chromatography system (Waldbronn, Germany), consisting of a binary pump (G1312A), an autosampler (G1367C) with thermostat, and a variable wavelength detector (G1315C) coupled to a SCIEX API 3200 triple quadrupole mass spectrometer (Applied Biosystems, Darmstadt, Germany). The latter was equipped with an electrospray ionization source (ESI), operating in the multiple reaction mode (MRM) with positive electrospray ionization (ESI^+). The ESI-MS conditions were as follows: ion spray voltage (IS) 3000 V; curtain gas (CUR) 25 psi; nebulizer gas 50 psi; heater gas 45 psi; temperature (T) 550 °C; declustering potential (DP) 66 V for AcLys-AcA and 41 V for AcLys-BDA; focusing potential (FP) 340 V; entrance potential (EP) 12 V for AcLys-AcA and 10.5 V for AcLys-BDA; collision cell entrance potential (CEP) 16 V for AcLys-AcA and 18 V for AcLys-BDA. HPLC conditions were as follows: Synergi Hydro-RP 4 μm polar RP 80 Å column (150 mm × 3 mm, Phenomenex, Torrance, California, USA) and a Synergi Aqua C18 guard column (4 μm); solvent system: A 0.1% formic acid, B acetonitrile; gradient profile: isocratic 5% B for 5 min, from 5 to 62% B over 6 min, from 62 to 95% B over 0.05 min, isocratic 95% B for 2.5 min, from 95 to 5% B over 0.05 min, and isocratic 5% B for 2.5 min; flow rate 600 μL/min; injection volume 10 μL; column oven temperature 30 °C. Samples were measured at concentrations of 0.001−50 μM and AcLys-BDA as internal standard with a final concentration of 1 μM added. Standards were diluted in water and the injection solution in the ratio of the HPLC solvent. Membrane filtered (0.45 μm) prior injection; retention times for both were 9.2 min. ESI^+-MS/MS in the MRM method in positive mode was used to detect AcLys-AcA as an analyte with the mass transition m/z 269.2/164.2 as a quantifier, after which m/z 269.2/84.1 and m/z 269.2/82.2 were used as qualifiers. In the case of the internal standard AcLys-BDA, the mass transition m/z 255.1/84.1 was used for quantification, while m/z 255.1/167.1 and m/z 255.1/209.2 were used to qualify the peak (see Table S6 and Figure S7).

The precision of the method 2.5 to 50,000 nM AcLys-AcA was determined by intraday (five replicate analyses of one concentration of AcLys-AcA in a row) and interday (one concentration of AcLys-AcA on 5 days in a row) repetition experiments; the coefficient of variation was 0.9% for intraday and 2.9% for interday experiments (see Table S7). The limit of detection (LOD) was determined as 1.6 nM, and the limit of quantification (LOQ) was 2.5 nM using a calibration approach (concentrations of AcLys-AcA 2.5 to 50,000 nM) adapted from the European Commission/Joint Research Centre Guidance Document (2023).[14]

Quantification of AcLys-AcA in Incubations with pRH. Quantification of AcLys-AcA in the incubations with pRH was performed with AcLys-BDA as an internal standard. The quantification was performed with an Agilent 1290 Infinity system equipped with a degasser (G1379B), binary pump (G4220A), autosampler (G4226A), and column oven (G1330B) (Agilent Technologies, Santa Clara, California, USA) coupled to a QTRAP 5500 mass spectrometer (Sciex, Darmstadt, Germany). The latter was equipped with an electrospray ionization source (ESI), operating in the multiple reaction mode (MRM) with positive electrospray ionization (ESI^+). The ESI-MS conditions were as follows: ion spray voltage (IS) 3000 V; curtain gas (CUR) 20 psi; nebulizer gas 50 psi; heater gas 60 psi; temperature (T) 550 °C; declustering potential (DP) 60 V for AcLys-AcA and AcLys-BDA; entrance potential (EP) 10 V for AcLys-AcA and AcLys-BDA; collision cell entrance potential (CEP) 16 V for AcLys-AcA and 18 V for AcLys-BDA. HPLC conditions were as follows: Synergi Hydro-RP 4 μm polar RP 80 Å column (150 mm × 3 mm, Phenomenex, Torrance, California, USA) and a Synergi Aqua C18 guard column (4 μm); solvent system: A 0.1% formic acid, B acetonitrile; gradient profile: isocratic 5% B for 5 min, from 5 to 62% B over 6 min, from 62 to 80% B over 0.05 min, isocratic 80% B for 2.0 min, from 80 to 32% B over 0.05 min, and isocratic 32% B for 2.5 min; back to 5% B in 0.55 min and isocratic for 1.5 min at 5% B; flow rate 600 μL/min; injection volume 1.0 μL; column oven temperature 30 °C. Other parameters see Supporting Information file. Samples measured at concentrations of 0.5−1000 nM and AcLys-BDA as internal standard with a final concentration of 1 μM added. Standards were diluted in water and the injection solution in the ratio of the HPLC solvent. Membrane filtered (0.45 μm) prior to injection; retention times for both were 7.8 min. ESI^+-MS/MS in the MRM method in positive mode was used to detect AcLys-AcA as an analyte with the mass transition m/z 269.2/164.2 as a quantifier, after which m/z 269.2/84.1 and m/z 269.2/82.2 were used as qualifiers. In the

https://doi.org/10.1021/acs.chemrestox.4c00083
Chem. Res. Toxicol. XXXX, XXX, XXX−XXX

case of the internal standard AcLys-BDA, the mass transition m/z 255.1/84.1 was used for quantification, while m/z 255.1/167.1 was used to qualify the peak (see Table S8 and Figure S8).

The precision of the method 0.5 to 1,000 nM AcLys-AcA was determined by intra- (five replicate analyses of one concentration of AcLys-AcA in a row) and interday (one concentration of AcLys-AcA on 5 days in a row) repetition experiments; the coefficient of variation was 0.8% for intraday and 1.8% for interday experiments (see Table S9). LOD was determined as 0.4 nM and LOQ as 0.5 nM using a calibration approach (concentrations of AcLys-AcA 0.5 to 1,000 nM) adapted from the European Commission/Joint Research Centre Guidance Document (2023).[14]

RESULTS

Oxidative ring opening as phase I of xenobiotic metabolism is known from the conversion of furan to BDA.[18] In literature, AcA was reported to be the primary phase I metabolite of 2-MF.[3,8] In general, α,β-unsaturated carbonyl compounds show a high reactivity toward nucleophilic cell components such as DNA and proteins, with thiol and amino groups being the favored targets.[19]

To investigate the formation of AcA indirectly, AcA was trapped with AcLys. The adduct as AcLys-AcA (Figure 1) was

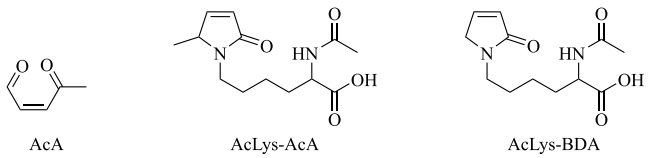

Figure 1. Structures of 3-acetylacrolein (AcA), postulated AcLys-AcA (AcA adduct with *N*-α-acetyl-L-lysine), and AcLys-BDA (butendial with *N*-α-acetyl-L-lysine).

synthesized and characterized, and two (U)HPLC-ESI$^+$-MS/MS methods were developed. The quantitative determination of AcA as AcLys-AcA was performed via (U)HPLC-MS/MS in MRM mode with AcLys-BDA as an internal standard, as shown in Figures S9 and S10.

The investigation of the reactivity of AcA with the reactants AcLys and AcCys was based on the conditions established before. The adduct formation to AcLy-AcA or AcCys-AcA was recorded after the addition of isolated AcA to the reactants AcCys and AcLys. Formed products were determined by HPLC-MS/MS. For AcLys and AcCys, adduct formation was concentration-dependent. The reaction rates were extremely rapid, showing completion within <1 min, with adduct yields stable for up to 24 h (Figure 2A/B). The results provided evidence that both amino acid derivatives could be suitable as potential scavenging reagents.

Metabolic Activation of 2-MF to AcA. Supersomes CYP 1A2, 2A6, 2C9, 2D6, 2E1, and 3A4 were commercially acquired. Here, a typical distribution of polymorphic CYPs (e.g., CYP 2C9*1 and CYP 2D6*1) was considered to represent the average metabolism.

Incubations of Supersomes with 2-MF (100 and 500 μM) for 10, 30, or 60 min were performed to identify the responsible enzym(s) converting 2-MF into AcA. Results are shown in Figure 3. CYP 2E1 was found to be a key enzyme within the tested Supersomes with a significant formation of AcA compared to the negative control, followed by a time- and dose-dependent increase.

For microsomal incubations, commercially available RLM and HLM were used. The RLM were derived from ~79 male

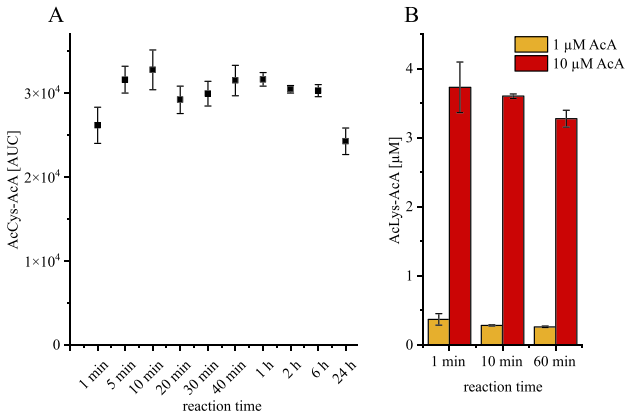

Figure 2. Reaction of AcA (1; 10 μM) with AcCys (4 mM) and AcLys (4 mM) as a function of incubation time. The reaction was carried out at 37 °C and 600 rpm. (A) Reaction of AcA (1 μM) with AcCys (4 mM) in water; AcCys-AcA is expressed as area under curve [AUC]. Detection of the AUC of AcCys-AcA using HPLC-ESI$^+$-MS/MS. (B) Reaction of AcA (1; 10 μM) with AcLys (4 mM) in K_2HPO_4 buffer (50 mM, pH 7.4), simulating the microsomal system. Detection of AcLys-AcA was performed by HPLC-ESI$^+$-MS/MS. n = 3, mean ± standard deviation. AcA: 3-acetylacrolein; AcCys: *N*-α-acetyl-L-cysteine, AcLys: *N*-α-acetyl-L-lysine.

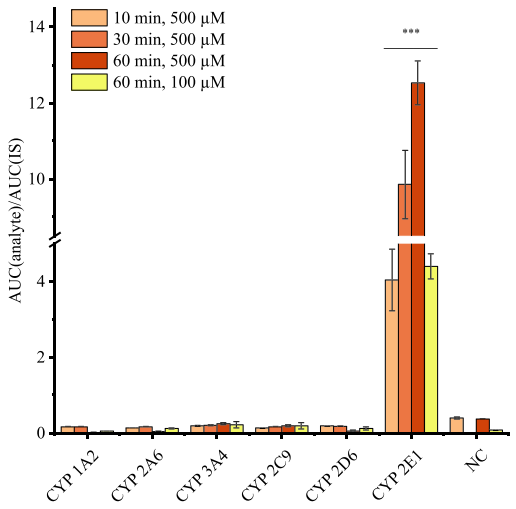

Figure 3. Incubation of the supersomes CYP 1A2, 2A6, 2C9, 2D6, 2E1, and 3A4 with 2-MF (100; 500 μM) for 10, 30, or 60 min to determine AcA formation. AcLys (4 mM) added as intercepting reagent. Detected as AcLys-AcA (analyte) with AcLys-BDA as internal standard (IS). n = 3−5, mean ± standard deviation, s significance tested against the negative control (NC, without NAPDH) using unpaired two-tailed t test with (*) $P < 0.05$ significant, (**) $P < 0.01$ highly significant, (***) $P < 0.001$ highly significant. AcA: 3-acetylacrolein, AcLys: *N*-α-acetyl-L-lysine, BDA: *cis*-2-butene-1,4-dial, CYP: cytochrome P450, 2-MF: 2-methylfuran.

Sprague−Dawley rats, whereas the HLM was derived from a broad pool of 150 male and female donors.

The linear range of the time-dependent conversion of 2-MF by RLM, HLM, and CYP 2E1 was determined at a constant 2-MF concentration (100 or 500 μM). They were separately incubated for 1−120 min, and the saturation of the enzyme capacity was recorded. An incubation time of 10 min was found to be suitable to operate in the linear range and at the

https://doi.org/10.1021/acs.chemrestox.4c00083
Chem. Res. Toxicol. XXXX, XXX, XXX−XXX

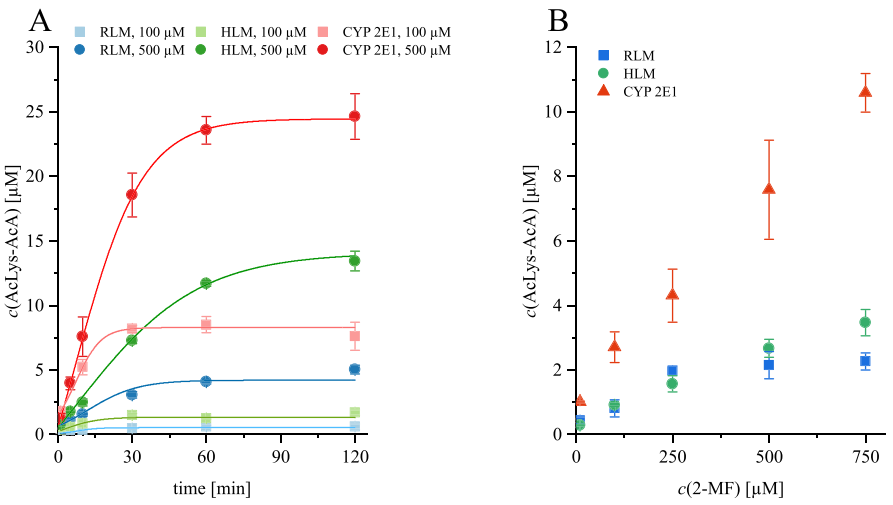

Figure 4. AcA formation in Supersome CYP 2E1 as well as RLM and HLM after incubation with 2-MF. AcLys (4 mM) added as intercepting reagent. (A) Time-dependent incubation (1−120 min) of CYP 2E1 with 100 and 500 μM 2-MF compared to that of RLM and HLM. (B) Dose-dependent incubation of CYP 2E1, RLM, and HLM (10 min, 10−750 μM 2-MF). AcA captured with AcLys and detected as AcLys-AcA. 120 nM CYP 2E1/mL or 1 mg microsomal protein/mL was used. n = 3−5, mean ± standard deviation, significance tested using unpaired two-tailed t test with (*) $P < 0.05$ significant, (**) $P < 0.01$ highly significant, (***) $P < 0.001$ highly significant. All values were tested as highly significant to the negative control (without NADPH, heat-inactivated enzymes). AcA: 3-acetylacrolein, AcLys: *N*-α-acetyl-L-lysine, CYP: cytochrome P450, HLM: human liver microsomes, 2-MF: 2-methylfuran, RLM: rat liver microsomes.

same time generate an adequate amount of product AcLys-AcA for detection. In the second step, the dose dependence of the 2-MF conversion (10−750 μM) was determined at a constant incubation time (10 min). These models described in the Materials and Methods section were used to determine the enzyme kinetic parameters. Finally, the conversion rate of 2-MF to AcA was analyzed, particularly with regard to the substrate concentrations used as shown in Figure 4.

The data indicated higher AcA formation in HLM in comparison to RLM. While AcA formation increased significantly with RLM, leveling out at 250 μM 2-MF, no saturation was observed with HLM and CYP 2E1 up to the highest concentration of 750 μM 2-MF. The highest AcA formation was observed with the CYP 2E1 incubation. When comparing the maximum turnover of 2-MF, it should be noted that microsomal incubations were performed with 1 mg of protein/mL, while individual enzymes were used at 120 nM CYP/mL providing a 6-fold higher activity of CYP 2E1 by Supersomes in comparison to HLM. Thus, the time- and dose-dependent formation of AcA as a reactive phase I metabolite of 2-MF by turnover with RLM, HLM, and CYP 2E1 as key enzyme (within the tested Supersomes selection) was demonstrated.

With the data achieved by incubation with RLM, HLM, and Supersomes CYP 2E1 enzyme kinetics were calculated and evaluated by Michaelis−Menten and Hill models (Figure 5).

The Michaelis−Menten constant K_m and the maximum reaction rate v_{max} or the change number k_{cat} for Supersomes were calculated as typical parameters. From this, the catalytic efficiency E_{cat} for CYP 2E1 and the *in vitro* intrinsic clearance CL_{int} were calculated.

The parameters derived from the data plotted according to the Michaelis−Menten-Hill model are shown in Figure 5. They model an approximation to the actual sample values, but the first criterion of convergence, in particular, was not achieved for all incubations. In addition, negative cooperativity was observed via the Hill factor ($n_H < 1$). This may be an indication of a biphasic enzyme reaction, which had to be checked using an Eadie-Hofstee plot.

The representation of the data in the Eadie-Hofstee diagram (Figure 6) showed different behaviors at different concentrations.

Figure 6 summarizes the enzyme kinetic parameters calculated in this way. All three enzyme systems showed a pattern of rapid metabolism at high substrate concentrations and a low maximum rate at low 2-MF concentrations. They can be categorized into sections of high affinity with low capacity (K_m small) and sections of low affinity with high capacity (K_m large). The two phases are indicated by the two equations that were the basis for the calculation of the kinetic quantities. It should be noted that the data based on a two-point equation (line II) should be treated with caution, especially at low concentrations. However, they provide a good approximation and are underpinned by reproducible occurrence in all three enzyme systems.

According to the prioritized criteria, Eadie-Hofstee is the model of choice for incubation with HLM and CYP 2E1. At high substrate concentrations with RLM, however, a weak correlative agreement was determined when including the four highest concentrations (values 1−4). The position of the straight lines in relation to each other also indicates a limited representation of the values by the model (see Figure 6). Although the exclusion of individual data points allows for a better interpretation, their exclusion cannot be statistically justified. Therefore, for the turnover of 2-MF with RLM K_m and v_{max} were derived conservatively from the Hill fit. However, the parameters are within the standard error of the values derived from the Eadie-Hofstee plot, which supports their representativeness.

Finally, the conversion rate to AcA was analyzed in relation to the amount of substrate 2-MF used in order to determine the influence of different substrate concentrations. For this purpose, the amount of AcA formed (nAcA) per amount of 2-

https://doi.org/10.1021/acs.chemrestox.4c00083
Chem. Res. Toxicol. XXXX, XXX, XXX−XXX

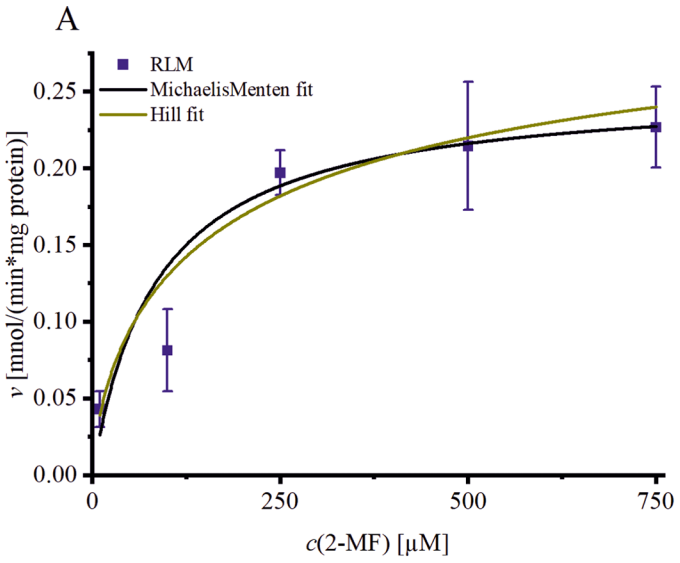

RLM

model	**michaelis menten**
equation	$y = v_{max} * x / (K_m + x)$
v_{max}	0.25 ± 0.04
K_m	85.86 ± 55.98
Chi square reduced	2.217
R square (COD)	0.931
cor. R square	0.908
model	**Hill**
equation	$y = v_{max} * x^n / (k^n + x^n)$
v_{max}	0.34 ± 0.22
k	194.57 ± 428.72
n	0.68 ± 0.35
Chi square reduced	2.404
R square (COD)	0.950
cor. R square	0.900

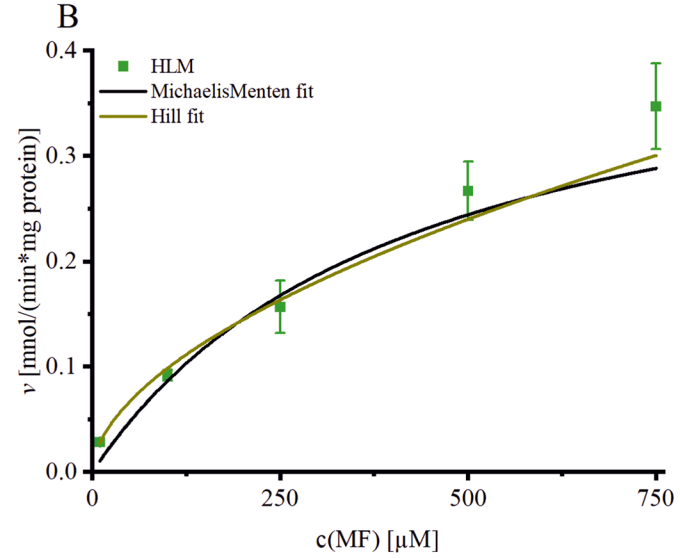

HLM

model	**michaelis menten**
equation	$y = v_{max} * x / (K_m + x)$
v_{max}	0.16 ± 0.05
K_m	50.40 ± 26.84
Chi square reduced	18.14
R square (COD)	0.822
cor. R square	0.726
model	**Hill**
equation	$y = v_{max} * x^n / (k^n + x^n)$
v_{max}	1679.71 ± 4860626.59
k	4.33e9 ± 2.26e13
n	0.55 ± 0.09
Chi square reduced	2.33
R square (COD)	0.985
cor. R square	0.969

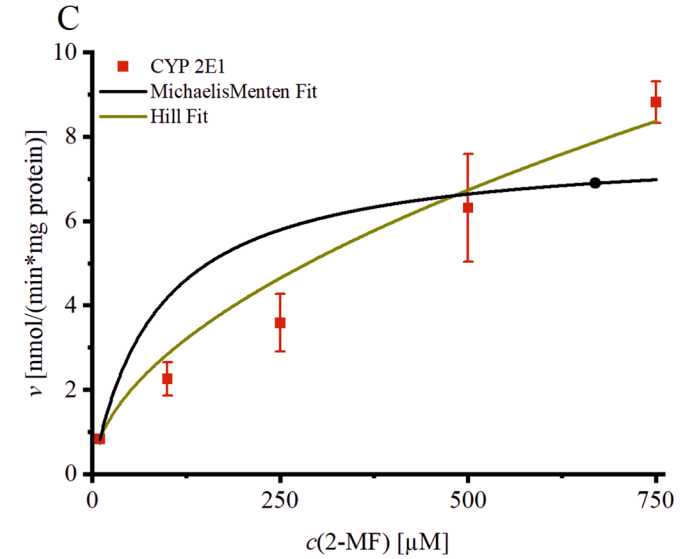

CYP 2E1

model	**michaelis menten**
equation	$y = v_{max} * x / (K_m + x)$
v_{max}	7.28 ± 2.06
K_m	85.72 ± 29.49
Chi square reduced	16.15
R square (COD)	0.839
cor. R square	0.785
model	**Hill**
equation	$y = v_{max} * x^n / (k^n + x^n)$
v_{max}	17960.80 ± 3.01e7
k	1.25e9 ± 3.93e12
n	0.54 ± 0.16
Chi square reduced	2.79
R square (COD)	0.981
cor. R square	0.963

Figure 5. Rate of formation of AcA by 2-MF incubation of RLM (A), HLM (B), and CYP 2E1 (C) in the Michaelis−Menten and Hill models. K_m; k: Michaelis−Menten constant, n: Hill factor; v_{max}: maximum rate of formation. AcA: 3-acetylacrolein, CYP: cytochrome P450, HLM: human liver microsomes, 2-MF: 2-methylfuran, RLM: rat liver microsomes.

https://doi.org/10.1021/acs.chemrestox.4c00083
Chem. Res. Toxicol. XXXX, XXX, XXX−XXX

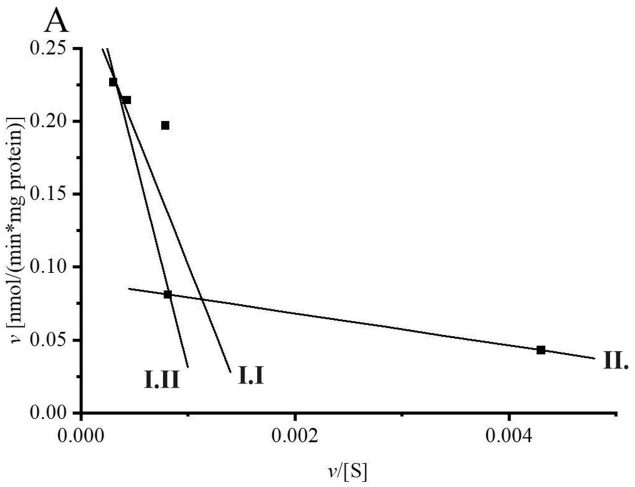

RLM

y = a+b*x	I.I	I.II	II.
a = v_{max}	0.30 ± 0.04	0.33 ± 0.03	0.09
−b = K_m	219.81.52 ± 81.52	299.89 ± 50.41	10.95
RSQ	1.2e−4	3.58e−4	
R square	0.707	0.973	
cor. R square	0.609	0.945	

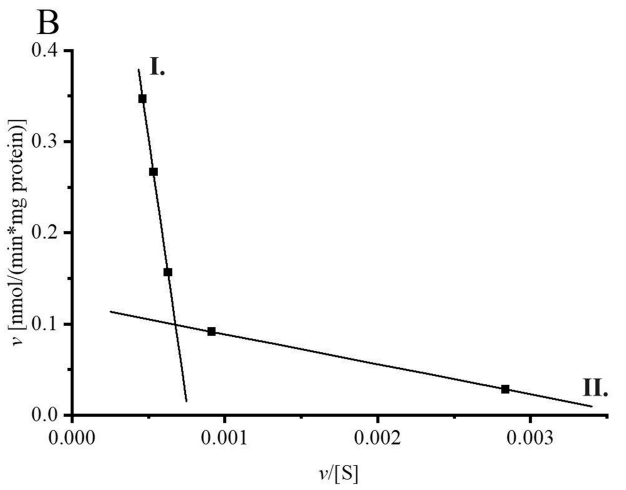

HLM

y = a+b*x	I.	II.
a = v_{max}	0.88 ± 0.006	0.12
−b = K_m	1156.34 ± 11.52	32.86
RSQ	1.8e−6	
R square	0.9999	
cor. R square	0.9998	

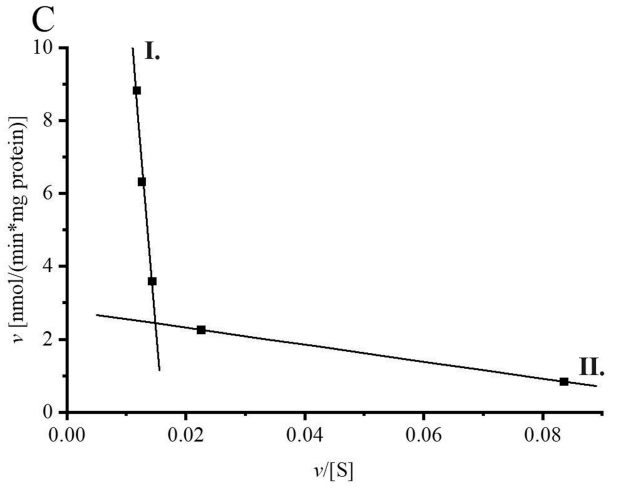

CYP 2E1

y = a+b*x	I.	II.
a = k_{cat}	31.36 ± 4.09	2.78
−b = K_m	1966.76 ± 315.37	23.29
RSQ	0.343	
R square	0.975	
cor. R square	0.950	

Figure 6. Eadie-Hofstee plots and derived parameters for AcA formation in RLM (A), HLM (B), and CYP 2E1 (C) after incubation with 10, 100, 250, 500, or 750 μM 2-MF. Parameters were determined as v_{max} for microsomes and kcat for supersomes. AcA: 3-acetylacrolein, CYP: cytochrome P450, HLM: human liver microsomes, 2-MF: 2-methylfuran, RLM: rat liver microsomes, and RSQ: residual sum of squares.

MF used (nMF) was plotted as a function of the dose in Figure 7.

In all three enzyme systems, the relative conversion in n-% was significantly highest at the lowest substrate concentration of 10 μM 2-MF. This was followed by a rapid drop in the conversion rate in the higher concentrations of 100−750 μM to a plateau. This can be due to the relative volatility of 2-MF at 37 °C, although the incubations were carried out in a closed system. A quantification of the 2-MF concentration over the incubation time was not included in these experiments. Furthermore, the AcA formed could also inhibit the conversion of 2-MF to AcA, and this could act as a so-called suicide substrate.

https://doi.org/10.1021/acs.chemrestox.4c00083
Chem. Res. Toxicol. XXXX, XXX, XXX−XXX

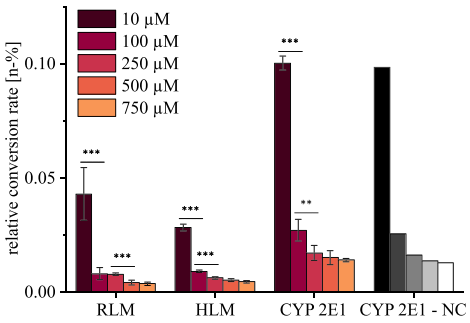

Figure 7. Relative conversion rate [n-%] of the enzymes to AcA in relation to the amount of substance 2-MF (10, 100, 250, 500, and 750 μM) used. Measured as AcLys-AcA. AcLys (4 mM) added as intercepting reagent. Comparison of RLM, HLM, CYP 2E1, and CYP 2E1 with deduction of the negative control (- NC). n = 3−5, mean ± standard deviation, significance tested using unpaired, two-sided t test with (*) $P < 0.05$ significant, (**) $P < 0.01$ highly significant, (***) $P < 0.001$ highly significant. AcA: 3-acetylacrolein, AcLys: *N*-α-acetyl-L-lysine, CYP: cytochrome P450, HLM: human liver microsomes, 2-MF: 2-methylfuran, RLM: rat liver microsomes.

***In Vitro* Formation of AcLys-AcA in Primary Rat Hepatocytes.** The aim was to analyze 2-MF and AcA in pRH with regard to potential biomarkers of exposure and effect. The possibly accompanying characterization of the cellular toxicokinetics could be used to prove AcA formation in pRH. For this purpose, pRH were incubated with 2-MF (10, 50, 100, 500, 1000 μM) or AcA (0.1, 0.5, 1, 5 μM) and the cell supernatant was analyzed after 1, 6, 18, 24, and 48 h as described in the Materials and Methods section. The potential formation of AcCys-AcA and AcLys-AcA was analyzed using the (U)HPLC-MS/MS methods. No evidence of AcCys-AcA formation was observed in the cell supernatants with 2-MF or AcA incubated pRH. In contrast to the observations regarding AcCys-AcA, the formation of AcLys-AcA in the cell supernatants of pRH was detected after incubation with both test substances. In the course of the validation of the SPE and HPLC-MS/MS methods, AcLys-BDA proved to be suitable as an internal standard for AcLys-AcA.

First, cytotoxicity in pRH was performed using 2-MF and AcA. At an incubation time of 24 h, the EC_{50} values were 551.1 ± 53.1 μM for 2-MF and 8.5 ± 1.3 μM for AcA.

When pRH were incubated with 2-MF, AcLys-AcA was detected in the cell supernatants in a time- and concentration-dependent manner (Figure 8A). After 1 h incubation with 100 μM 2-MF a significant increase in the adduct compared to the negative control was shown, while from 6 h, 50 μM 2-MF already led to a significant difference. The concentration dependence existed at all time points, tested between 10 and 1000 μM, or 100 μM at 6 h (deviating test due to the high standard deviation in the two highest concentrations).

Incubation of pRH with the metabolite AcA and the formation of AcLys-AcA are shown in Figure 8B. The formation is also time- and dose-dependent. After 48 h of incubation with 0.5 μM AcA the amount of AcLys-AcA differed significantly from the negative control. However, 5 μM AcA led to a highly significant increase in adduct levels compared to the negative control at all time points and showed a concentration dependence (versus 0.1 μM) as well as time dependence (1 h versus 6 h, 24 h versus 48 h). The significant change over a period of 2 days (48 h) initially appears surprising for a reaction characterized chemically (data not

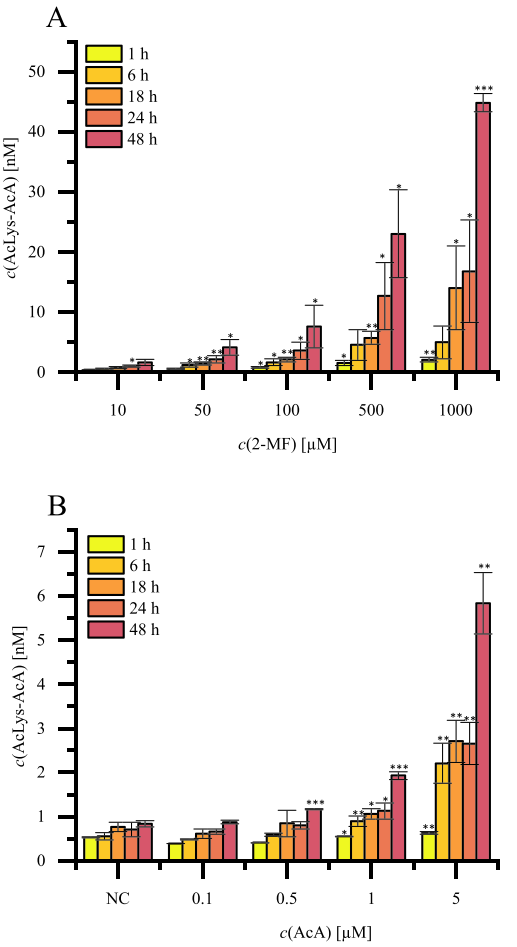

Figure 8. Formation of AcLys-AcA [nM] in pRH after incubation with (A) 2-MF (10−1000 μM) and (B) AcA (0.1−5 μM). Significances were tested against the negative control (NC; DMSO 0.1%) by one-sided t test. n = 3−5, mean ± standard deviation, significances tested by unpaired, one-sided t test with (*) $P < 0.05$ significant, (**) $P < 0.01$ highly significant, (***) $P < 0.001$ highly significant. AcA: 3-acetylacrolein, AcLys: *N*-α-acetyl-L-lysine, 2-MF: 2-methylfuran, pRH: primary rat hepatocytes.

shown). However, the cellular processes *in vitro* certainly take time. This includes absorption into and elimination from the cell but also the degradation of peptides (or proteins) with bound AcA to AcLys-AcA. The elimination time can therefore vary depending on the step.

A time- and dose-dependent formation in pRH was observed. Interestingly, AcLys-AcA was present in the negative controls (NC) as well. Additionally, cells were incubated for different time points in pure culture medium without 2-MF or AcA, and adducts were formed. A cross-contamination could be excluded. Since no adducts were detectable in pure culture medium without cells, the question arose about endogenous formation of AcLys-AcA in untreated pRH.

In addition, the substance-related conversion rate (in parts per million) was calculated as the amount of AcLys-AcA formed in relation to the corresponding amount of 2-MF or AcA used. Parts A and B of Figure 9 initially describe the conversion rate without consideration of the negative control (NC) of AcLys-AcA as antiproportional to the substrate used at all time points. If the NC was subtracted from the sample

https://doi.org/10.1021/acs.chemrestox.4c00083
Chem. Res. Toxicol. XXXX, XXX, XXX−XXX

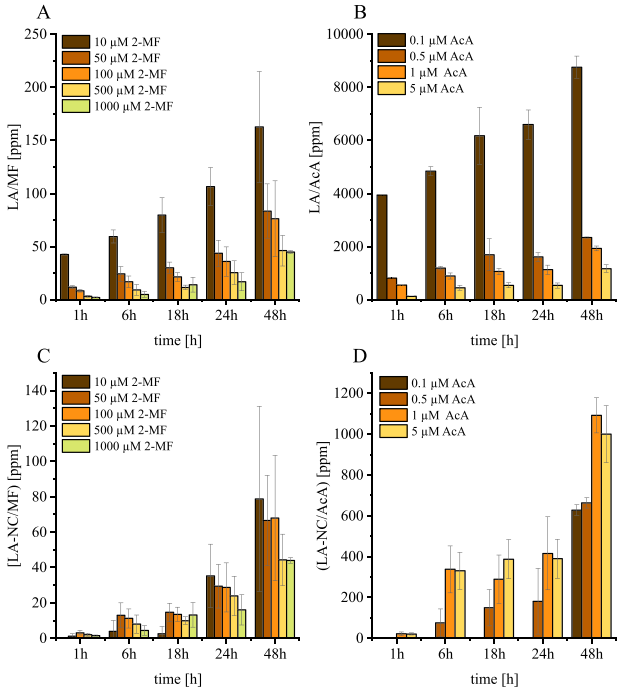

Figure 9. Relative conversion rates (ppm) to AcLys-AcA (LA) in pRH (1−48 h) in relation to the amount of substance used, 2-MF (10−1000 μM; (A, C) and AcA (0.1−5 μM; (B, D), without (A, B) and with (C, D) subtraction of the negative control (NC; DMSO, 0.1%). AcLys (4 mM) added as intercepting reagent. n = 3−5, mean ± standard deviation. AcA: 3-acetylacrolein, AcLys: *N*-α-acetyl-L-lysine, 2-MF: 2-methylfuran, pRH: primary rat hepatocytes.

value, as shown in parts C and D of Figure 9, the influence of the NC on the conversion rate became apparent.

By standardization to the amount of substrate used, no significant difference between the 2-MF concentrations (Figure 9C) was determined. Only a tendency toward reduced formation with increasing concentration was observed. However, the interpretation as an inhibitory effect on the metabolizing enzymes, as described before, can only be surmised here. With regard to the change in the conversion rate over time, it is more likely to be a trend toward an increase. The same is also recognizable in the case of the conversion rate from AcA to AcLys-AcA excluding the negative control (Figure 9D). This could, for example, be due to a delayed elimination of AcLys-AcA from the cell into the cell supernatant.

In general, AcLys-AcA qualifies as a potential biomarker. In addition, the results showed that AcA was indeed formed at the cellular level after the 2-MF exposure.

DISCUSSION

The synthesized products AcCys-AcA and AcLys-BDA were identified and characterized via NMR and MS. The occurrence of AcLys-AcA as (presumed) isomers, which could not be separated semipreparatively such as AcLys-BDA, made characterization via NMR more challenging. Mass spectrometric investigations of the synthesis product of AcLys with AcA supported the reaction of the ε-amino group of AcLys with a carbonyl group of AcA with subsequent ring closure and water cleavage. This was consistent with a hypothesis from reference literature that AcA reacted in a similar manner to BDA.[13] The mass difference between the molecular ions and fragments of AcLys-AcA and AcLys-BDA was 15 Da, which corresponded to the mass of a methyl group. The intensities of the fragments, which were reflected in the ratio of the mass transitions, also matched. Verification by NMR showed that the adduct is unstable in organic solvents or that a rearrangement occurred. Measurements in D_2O showed two important facts: First, all signals except for the expected vinyl structural units of the pyrrole ring were assigned, and second, based on the integrals, two components were assumed. It was hypothesized that the exchangeable protons in D_2O were not visible due to hydration with D_2O. Using DOSY (see Supporting Information Figure S11), the diffusion coefficients of the ^1H signals of the underlying protons were used to show that if several compounds are present in D_2O, they are structurally very similar (as is the case for isomers, for example). The subsequent elemental analysis allowed a normalized ratio of 1:1.2 to be derived for AcLys-AcA and H_2O, assuming the chemical formula and molar mass from the mass spectrometric measurements. The exact mass of AcLys-AcA and its fragmentation were checked in high-resolution scans and specifically evaluated for hydrated forms. Simple hydration with an additional mass of 18 Da was not detected. This does not rule out the hypothesis that water accumulated on AcLys-AcA. Thus, the product can be detectable by mass spectrometry as free AcLys-AcA, and, at the same time, the NMR signals would be superimposed on the pyrrolic ring of the adduct. The nonequimolar amount of water to AcLys-AcA present in the elemental analysis rather speaks in favor of an accumulation than a covalent binding. As a consequence, all approaches for further experiments with AcLys-AcA were carried out in water, where the signals of the NMR and MS measurements proved to be stable. HPLC-ESI$^+$-MS/MS experiments showed the same m/z and fragmentation pattern for two signals, AcLys-AcA I and II, which eluted at R_t = 8.6 and 9.2 min. When the synthesis was separated semi-preparatively, the fractions always showed the same ratio of 10:1 of I to II, regardless of their partitioning. This suggested the presence of the two forms in equilibrium. The equilibrium hypothesis is supported by the observation that the same ratio of AcLys-AcA I and II was present in the reaction of AcLys with isolated AcA (from MF oxidation with DMDO), enzymatically generated AcA (microsome incubations), and AcA formed *in vitro* by pRH. In addition to the purely practical impossibility of separating AcLys-AcA I and II, the occurrence of the two products in the real also argued in favor of a joint isolation of AcLys-AcA I and II. It allowed the development of a robust, sensitive, and specific method to analyze the adduct of AcA with AcLys.

Studies with ^{14}C-labeled 2-MF identified the liver as the main target organ in accordance with histopathological examinations.[10,11] In this study, liver microsomes were used to verify AcA as a metabolite, the formation of which had previously only been determined indirectly via the protein-bound radioactivity of ^{14}C-labeled 2-MF. In addition, potential interspecies differences between human (HLM) versus rat liver microsomes (RLM) were investigated together with the identification of the prime isoenzyme(s) responsible for the metabolic conversion.[23−25]

Within the tested Supersomes, CYP 2E1 was found to be the key enzyme for the conversion of 2-MF to AcA in the test system. A final concentration of 120 nM CYP 2E1 corresponded to 12 pmol per incubation batch (V = 100

https://doi.org/10.1021/acs.chemrestox.4c00083
Chem. Res. Toxicol. XXXX, XXX, XXX−XXX

Table 1. Enzyme kinetic parameters of AcA formation. Own results and data from the literature. In the biphasic system, (I) stands for the reaction at high substrate concentrations (250, 500, and 750 μM) and (II) for the reaction at low substrate concentrations (10 and 100 μM)

Substrate	test system	v_{max}|k_{cat} [a] [μmol/(mg prot.·min)] [μmol/(μmol CYP·min)]	K_M [μM]	CL_{int} | E_{cat} [#]
Own data: AcA adducts (HPLC-MS/MS) after microsomal incubations (10−750 μM 2-MF)				
2-MF	RLM, untr.	I) 0.34; II) 0.09	I) 194.57; II) 10.95	I) 1.7e-3; II) 8.2e-3
	HLM	I) 0.88; II) 0.12	I) 1156.34; II) 32.86	I) 7.6e-4; II) 3.6e-3
	CYP 2E1	I) 31.68; II) 2.78	I) 1966.76; II) 23.29	I)1.6e-2; II) 1.1e-1
Ravindranath and Boyd (1985):[9] Micosomal bound radioactive signal after ^{14}C-MF (2.5−20 mM total 2-MF)				
2-MF	RLM, untr.	0.27	1417	1.9e-4
	RLM, pretr.	0.41	463	8.9e-4
Peterson et al. (2005):[32] BDA adducts (HLPC-MS/MS) after microsomal incubations (10−500 μM)				
Furan	RLM, untr.	0.0025 ± 0.1	37.6 ± 4.3	6.6e-5
	RLM, pretr..	0.0059 ± 0.5	18.5 ± 6.8	3.2e-4
	CYP 2E1	26	65.1 ± 16.4	3.9e-1
Gates et al. (2012[30]): BDA adducts (HPLC-MS/MS) after microsomal incubations (LM: 50 μM furan, CYPs: 20 oder 400 μM furan)				
Furan	RLM, untr.	0.0016		
	HLM	0.0013		
	CYP 2E1	34 ± 4	24 ± 13	1.4

[a]Microsomes from phenobarbital pretreated rats. For better comparability, literature values have been converted to the appropriate unit and rounded where necessary. CYP: cytochrome P450, HLM: human liver microsomes, LM: liver microsomes, 2-MF: 2-methylfuran, RLM: rat liver microsomes, untreated: untreated rats, pretreated: pretreated rats.

μL). This equaled 2 ± 1.3 pmol CYP 2E1 in HLM incubations, assuming 20 ± 13 pmol CYP 2E1/mg protein in HLM.[20] The 6-fold increase in the amount of CYP 2E1 in the Supersome experiment is reflected in the reduced AcA formation when incubated with HLM. According to the manufacturer's instructions, a 6-fold higher catalytic activity is to be expected with Supersomes compared to HLM, which was confirmed here.

Incubation (120 min) of HLM with 2-MF (500 μM) produced a 3-fold higher level of AcA compared to that of RLM, although 1 mg of microsomal protein/mL was used in each case. This raises the question of a species-specific difference. Comparing CYP 2E1 activity Shimada et al. (1994)[20] observed a 1.7−4.2-fold higher oxidation rate in HLM (696 ± 986 pmol product/(mg protein/min)) than in RLM (403 ± 57 pmol product/(mg protein/min)). However, the standard deviations illustrate the large turnover range of CYP 2E1 activity in HLM, especially in contrast to standardized laboratory conditions from which the RLM originate. On the one hand, environmental and lifestyle factors have an effect on CYP 2E1 expression or activity.[21] On the other hand, polymorphisms for CYP 2E1 are known to play a decisive role in the metabolism of drugs or toxins depending on ethnic origin.[22] CYP 2E1 is responsible for the monooxygenation of xenobiotic substances such as *N*-nitrosamines, benzene, and alcohols.[26−29] Thus, the comparison of HLM and CYP 2E1 in this study, which represent the average activity but do not cover the entire range of variability in HLM, does not, per se, indicate a species-specific difference between humans and rats.

The first microsomal 2-MF incubations in combination with semicarbazide as an intercepting reagent have been described in the literature in order to detect the formation of a reactive metabolite as disemicarbazone.[8,9] In the following microsomal incubations from partially pretreated rats, the radioactivity bound to microsomal protein (isolated) was determined after incubation with ^{14}C-2-MF. The binding of ^{14}C-labeled material to isolated protein was equated to the quantitative conversion of 2-MF to the reactive metabolite. The importance of the CYP enzymes for 2-MF metabolism associated with the influence of CYP inducers and inhibitors was confirmed here. Qualitatively, an analogy can also be drawn here with the metabolic activation of furan to BDA via CYP 2E1.[19,30,31] Oxidative ring opening to the reactive α,β-unsaturated carbonyl compound was also detected by using a scavenging reagent in HLM, RLM, and mouse liver microsomes. CYP 2E1 was also identified as the key enzyme for BDA formation from furan in the same study.[30] These findings reinforce the hypothesis that 2-MF is subject to a similar metabolism as furan, which is crucial for comparisons in risk assessment.

The concentration-dependent measurements of AcA formation from the 10 min incubation of 2-MF in RLM, HLM, and CYP 2E1 formed the basis for the calculation of enzyme kinetic parameters. The Michaelis−Menten constant K_M and the maximum reaction rate v_{max} or the change number k_{cat} for Supersomes were calculated as typical parameters.

Using kinetic parameters, the maximum velocity indicates effective oxidative ring opening of 2-MF to AcA by RLM, HLM, and CYP 2E1 (Figure 6). The kinetic parameters are summarized in Table 1 and compared to data available from the literature.

Ravindranath and Boyd (1985)[9] determined a v_{max} = 0.53 μmol/2 mg microsomal protein/min with K_M = 1.417 mM by plotting the data in the Eadie-Hofstee diagram from the incubation RLM from untreated rats. When the rats were pretreated with phenobarbital, a v_{max} = 0.81 μmol/2 mg microsomal protein/min and K_M = 0.463 mM was achieved. The total 2-MF concentration of 2.5−20 mM was higher than the concentrations used in this study. Nevertheless, the parameters in Table 1 show comparable v_{max} (0.27; and 0.41 μmol/(mg prot./min) of untreated and pretreated RLM, respectively) with the high concentration range of our own measurements (0.34 μmol/(mg prot./min)). The parameter K_M also aligns with the high concentration used by Ravindranath and Boyd (1985).[9] It is important to note that this is again an indirect measurement of a reactive metabolite

https://doi.org/10.1021/acs.chemrestox.4c00083
Chem. Res. Toxicol. XXXX, XXX, XXX−XXX

as the amount of radiolabeled material bound to an isolated microsomal protein. In contrast, in the present work, AcA was captured with AcLys and the specific adduct (AcLys-AcA) was detected directly. This reflects the freely accessible AcA that has the potential to react with the cellular components. For the assessment of toxicodynamics and kinetics, the freely available AcA, which is not bound to microsomal protein, provides an advantageous statement. However, the inactivation and further depletion of CYP through the binding of AcA (as a suicide substrate) can be important for the further metabolism of other xenobiotics.

For comparison, the microsomal conversion of furan to BDA is also presented in Table 1. In both cited literature here, RLM, HLM, and CYP(s) were incubated with furan. The reactive intermediate BDA was detected in the presence of an excess of AcLys and AcCys as a conjugate via HPLC-MS/MS. Incubation with untreated/treated RLM and HLM resulted in significantly lower reaction rates than for 2-MF. This applied to incubation ranges of 10−500 μM furan.[30,32] Incubation of various CYPs with 20 or 400 μM furan characterized CYP 2E1 with K_M = 24 ± 13 μM and v_{max} = 34 ± 4 pmol BDA/pmol CYP/min as the key enzyme for the metabolic activation of furan.[30] Thus, the constant K_M of furan was in the range of the K_M of low substrate concentration of 2-MF (own measurements), while the change number k_{cat} (furan) corresponded to the k_{cat} of 2-MF (own measurements) at high substrate concentration. Since only two incubation concentrations were selected for furan,[30] no comparison regarding to biphasic reaction kinetics is possible here.

In all three enzyme systems (HLM, RLM, and CYP 2E1), the relative conversion in n-% was highest at the lowest substrate concentration of 10 μM 2-MF. This was followed by a rapid drop in the conversion rate in the higher concentrations of 100−50 μM to a plateau. Ravindranath et al. (1984)[8] also described the inhibition of metabolism from 500 μM, which was noticeable by no binding of ^{14}C-labeled material to isolated microsomal protein. Following the same measurement principle, furan was described as a suicide substrate.[33]

We hypothesized that AcCys-AcA could be formed as a reaction product after exposure to AcA or metabolic activation of 2-MF in pRH. Adducts of AcCys could hypothetically be formed directly or via the degradation of GSH adducts to mercapturic acid, as is the case for acrylamide or acrolein reported before.[34] However, this hypothesis was not confirmed experimentally here. Additional investigations by our group showed no depletion of GSH in pRH or HepG2 cells after exposure to 2-MF (data not shown). This suggests that conjugation to GSH is not the primary detoxification step for AcA. In contrast, the formation of GSH-BDA adducts upon furan exposure is known both *in vitro* and *in vivo*.[19,35−37] Recently, Li and co-workers used an approach to identify covalently protein bound furan, 2-MF, and 2,5-DMF metabolites in mouse primary hepatocytes.[38] They observed 171 lysine-based and 145 cysteine-based adducts using a chemoproteomic platform, indicating a binding affinity of those metabolites to proteins and possible protein modifications occurring.

To our surprise, during the incubations of pRH with AcA and 2-MF, AcLys-AcA was present in the negative controls, as well. A hypothetical endogenous source could be connected to lipid peroxidation (LPO). LPO may not only produce 2-MF[39] but also AcA or 2-oxo-4-alkenyl.[40,41] Thus, formation of AcA and its precursors, especially from the breakdown of fatty acids, might be possible. The isolation and cultivation of pRH represent a stressful situation for the organoid-grown hepatocytes, which is evident in the limited lifespan (at maximum 72 h). Oxidative stress with lipid peroxidation could therefore be a hypothetical cause for the observed formation of AcLys-AcA in the negative controls. In model experiments, α,β-unsaturated carbonyl compounds formed in the course of lipid oxidation formed 2-MF, whereby amino acids or pro-oxidative copper ions had a catalytic effect. Intramolecular cyclization of the 4-hydroxyalkenals represented an intermediate step.[39,42]

The fact that in incubation of pRH with 2-MF and AcA the same adducts are built supports the evidence concerning the metabolism of 2-MF to AcA *in vitro*.

Human urine after coffee consumption (as 2-MF-containing food) was analyzed for potential biomarkers in two intervention studies by our group. In untargeted measurements, time-dependent excretion of the adduct AcLys-AcA was observed. However, since the uptake of 2-MF was not known in the study, no statement was made here about the correlation between the uptake of 2-MF and the excretion of AcLys-AcA.[35] The hypothesis of AcLys-AcA as an actual biomarker of 2-MF was tested in a human study with defined 2-MF intake.[37] As already shown by Kremer and co-workers, AcLys-AcA and Lys-AcA were formed from 2-MF in addition to Lys-BDA, AcLys-BDA, and GSH-BDA from furan.[36] Gates et al. (2014) semiquantitatively described the formation of AcLsy-BDA in the medium of hepatocytes from rats, mice, and human samples.[31] They also demonstrated the multiple adduct formation of BDA with GSH in combination with other binding partners, such as lysine or glutamine. The reactivity of AcA will be different from that of BDA, due to the acetyl group instead of a second aldehyde group. This may be due to the influence on the range of the nucleophilic biopartners of preference. Therefore, further studies on an extended range of biomarkers are indicated. Moreover, endogenous formation of 2-MF metabolites via, e.g., lipid peroxidation should be ascertained and this endogenous background be taken into consideration for risk assessment purposes.

CONCLUSION

AcA was characterized as a reactive metabolite of 2-MF *in vitro* as well as its adducts with nucleophilic cellular components.

The metabolic activation of 2-MF to AcA was confirmed in RLM and demonstrated for the first time in HLM. Oxidative ring opening of 2-MF, primarily mediated by CYP 2E1, was shown in Supersomes (CYP 1A2, 2A6, 2C9, 2D6, 2E1, 3A4). The lysine adduct, AcLys-AcA, was characterized as a potential 2-MF exposure biomarker, while the cysteine adduct AcCys-AcA was not detected. The relative conversion rate in relation to the substrate concentration used indicates an inhibitory effect of 2-MF, which may characterize 2-MF as a suicide substrate for CYP450. These results may contribute data for the risk assessment of 2-MF in the future.

ASSOCIATED CONTENT

Supporting Information

The Supporting Information is available free of charge at https://pubs.acs.org/doi/10.1021/acs.chemrestox.4c00083.

Figure S1: ^{1}H NMR spectrum of AcLys-AcA in D_2O (600 MHz). Table S1: ^{1}H NMR signals of AcLys-AcA and AcLys in D_2O with structural assignment of

https://doi.org/10.1021/acs.chemrestox.4c00083
Chem. Res. Toxicol. XXXX, XXX, XXX−XXX

spectrum from figure S1. Figure S2: HPLC-ESI$^+$-MS^2 spectrum of AcLys-AcA with postulated fragmentation pattern. Figure S3: ^{1}H NMR spectrum (600 MHz) of AcCys-AcA in D_2O. Table S2: ^{1}H- and ^{13}C NMR signals of AcCys-AcA with structural assignment, see Figure S3. Figure S4: HPLC-ESI$^+$-MS^2 spectrum of AcCys-AcA with postulated fragmentation pattern. Figure S5: ^{1}H NMR spectrum of AcLys-BDA in DMSO-d_6 (600 MHz). Table S3: ^{1}H- and ^{13}C NMR signals of AcLys-BDA in DMSO-d_6 (at 600 MHz. respectively 151 MHz). Figure S6: HPLC-ESI$^+$-MS^2 spectrum of AcLys-BDA with postulated fragmentation pattern. Table S4: Solutions for incubations with microsomes and Supersomes. Table S5: Incubations of microsomes or Supersomes. Table S6: MS parameters for quantification of AcLys-AcA with AcLys-BDA (method I). Figure S7: HPLC-ESI$^+$-MS/MS chromatogram (MRM mode) of (A) AcLys-AcA (1 μM) and (B) AcLys-BDA (1 μM). Table S7: Calibration of AcLys-AcA with validation parameters. Table S8: MS parameters for quantification of AcLys-AcA with AcLys-BDA (method II). Figure S8: Regression line of the calibration series of AcLys-AcA (2.5−1000 nM) for method I. Table S9: Calibration of AcLys-AcA with validation parameters. Figure. S9: HPLC-ESI$^+$-MS/MS chromatogram (MRM mode) of AcLys-AcA (A) and AcLys-BDA (B) with method II. Figure S10: Regression line of the calibration series of AcLys-AcA (0.5−1000 nM) for method. II Figure S11: DOSY measurements of AcLys-AcA in (A) D_2O and (B) DMSO-d_6 (PDF)

AUTHOR INFORMATION

Corresponding Author

Elke Richling − *Department of Chemistry, Division of Food Chemistry and Toxicology, University of Kaiserslautern-Landau, Kaiserslautern 67663, Germany;* orcid.org/0000-0001-5746-8032; Email: elke.richling@chem.rptu.de; Fax: (+49)6312053085

Authors

Verena Schäfer − *Department of Chemistry, Division of Food Chemistry and Toxicology, University of Kaiserslautern-Landau, Kaiserslautern 67663, Germany*

Simone Stegmüller − *Department of Chemistry, Division of Food Chemistry and Toxicology, University of Kaiserslautern-Landau, Kaiserslautern 67663, Germany*

Hanna Becker − *Department of Chemistry, Division of Food Chemistry and Toxicology, University of Kaiserslautern-Landau, Kaiserslautern 67663, Germany*

Complete contact information is available at: https://pubs.acs.org/10.1021/acs.chemrestox.4c00083

Author Contributions

The manuscript was written through contributions of all authors. All authors have given approval to the final version of the manuscript.

Funding

This research was funded by the Deutsche Forschungsgemeinschaft (DFG) project numbers RI 1176/12-1 and RI 1176/13-1 and by the EU-INTERREG project BIOVAL supported by the European Funds for Regional Development, project no. 018-4-09-021.

Notes

The authors declare no competing financial interest.

ACKNOWLEDGMENTS

We thank Janina Leidner for her support in preparing rat hepatocytes. Special thanks to Dr. Harald Kelm, Christiane Müller, Dr. Sarah Reeb, and Dr. Daniel Bellaire for support with NMR measurement and spectra evaluation and Ruth Bergsträßer for elementary analysis. Further we thank Prof. Dr. Gerhard Eisenbrand for scientific discussions.

ABBREVIATIONS

2,5-DMF, 2,5-dimethylfuran; 2-MF, 2-methylfuran; AcA, 3-acetyl acrolein; AcCys, *N*-α-acetyl-L-cysteine; AcLys, *N*-α-acetyl-L-lysine; BDA, *cis*-2-butene-2,4-dial; CYP, cytochrome P 450 enzyme; NC, negative control; RLM, rat liver microsomes; HLM, human liver microsomes, RLM rat liver microsomes, pRH, primary rat hepatocytes; SD, standard deviation; SIDA, stabil isotope dilution analysis; IS, internal standard

REFERENCES

(1) Knutsen, H. K.; Alexander, J.; Barregård, L.; Bignami, M.; Brüschweiler, B.; Ceccatelli, S.; et al. Risks for public health related to the presence of furan and methylfurans in food. *EFSA* **2017**, *15* (10), 11058.

(2) Fromberg, A.; Mariotti, M. S.; Pedreschi, F.; Fagt, S.; Granby, K. Furan and alkylated furans in heat processed food, including home cooked products. *Czech J. Food Sci.* **2014**, *32*, 443−448.

(3) Becalski, A.; Halldorson, T.; Hayward, S.; Roscoe, V. Furan, 2-methylfuran and 3-methylfuran in coffee on the Canadian market. *J. Food Compost. Anal.* **2016**, *47*, 113−119.

(4) Rahn, A.; Yeretzian, C. Impact of consumer behavior on furan and furan-derivative exposure during coffee consumption. A comparison between brewing methods and drinking preferences. *Food Chem.* **2019**, *272*, 514−522.

(5) Habibi, H.; Mohammadi, A.; Hoseini, H.; Mohammadi, M.; Azadniya, E. Headspace liquid-phase Microextraction followed by gas chromatography-mass spectrometry for determination of furanic compounds in baby foods and method optimization using response surface methodology. *Food Anal. Methods* **2013**, *6* (4), 1056−1064.

(6) Lipinski, S.; Lindekamp, N.; Funck, N.; Cramer, B.; Humpf, H.-U. Determination of furan and alkylfuran in breakfast cereals from the European market and their correlation with acrylamide levels. *Eur. Food Res. Technol.* **2024**, *250*, 167−180.

(7) Sirica, A. E.; Radaeva, S.; Caran, N. NEU overexpression in the furan rat model of cholangiocarcinogenesis compared with biliary ductal cell hyperplasia. *Am. J. Pathol.* **1997**, *151*, 1685−1694.

(8) Ravindranath, V.; Burka, L.; Boyd, M. Reactive metabolites from the bioactivation of toxic methylfurans. *Science* **1984**, *224* (4651), 884−886.

(9) Ravindranath, V.; Boyd, M. R. Metabolic activation of 2-methylfuran by rat microsomal systems. *Toxicol. Appl. Pharmacol.* **1985**, *78* (3), 370−376.

(10) Ravindranath, V.; McMenamin, J. H.; Dees, J. H.; Boyd, M. R. 2-Methylfuran toxicity in rats? Role of metabolic activation in vivo. *Toxicol. Appl. Pharmacol.* **1986**, *85* (1), 78−91.

(11) Gill, S. S.; Kavanagh, M.; Cherry, W.; Barker, M.; Weld, M.; Cooke, G. M. A 28-day gavage toxicity study in male Fischer 344 rats with 2-methylfuran. *Toxicol. Pathol.* **2014**, *42* (2), 352−360.

(12) Adam, W.; Bialas, J.; Hadjiarapoglou, L. Kurzmitteilung/Short Communication A Convenient Preparation of Acetone Solutions of Dimethyldioxirane. *Chem. Ber.* **1991**, *124* (10), 2377.

(13) Chen, L. J.; Hecht, S. S.; Peterson, L. A. Characterization of amino acid and glutathione adducts of cis-2-butene-1,4-dial, a reactive metabolite of furan. *Chem. Res. Toxicol.* **1997**, *10* (8), 866−874.

(14) European Commission/Joint Research Centre Guidance Document on Pesticide Analytical Methods for Risk Assessment

and Post-approval Control and Monitoring Purposes. *SANTE/2020/12830*, Rev.2; Supersedes Guidance Documents SANCO/3029/99 and SANCO/825/00; EU Commission Services, 2023.
(15) Schrenk, D.; Karger, A.; Lipp, H.-P.; Bock, W. 2,3,7,8-Tetrachlorodibenzo-p-dioxin and ethinylestradiol as co-mitogens in cultured rat hepatocytes. *Carcinogenesis* **1992**, *13* (3), 453−456.
(16) Page, B.; Page, M.; Noel, C. A new fluorometric assay for cytotoxicity measurements in vitro. *Int. J. Oncol.* **1993**, *3* (3), 473−476.
(17) Schäfer, V.; Stegmüller, S.; Becker, H.; Richling, E. Reactivity of the 2-methylfuran phase I metabolite acetylacrolein towards DNA. *J. Agric. Food Chem.* submitted.
(18) Moro, S.; Chipman, J. K.; Wegener, J.-W.; Hamberger, C.; Dekant, W.; Mally, A. Furan in heat-treated foods: Formation, exposure, toxicity, and aspects of risk assessment. *Mol. Nutr. Food Res.* **2012**, *56*, 1197−1211.
(19) Peterson, L. A.; Cummings, M. E.; Chan, J. Y.; Vu, C. C.; Matter, B. A. Identification of a cis-2-butene-1,4-dial-derived glutathione conjugate in the urine of furan-treated rats. *Chem. Res. Toxicol.* **2006**, *19* (9), 1138−1141.
(20) Shimada, T.; Yamazaki, H.; Mimura, M.; Inui, Y.; Guengerich, F. P. Interindividual variations in human liver cytochrome P-450 enzymes involved in the oxidation of drugs, carcinogens and toxic chemicals: studies with liver microsomes of 30 Japanese and 30 Caucasians. *J. Pharmacol. Exp. Ther.* **1994**, *270* (1), 414−423. https://jpet.aspetjournals.org/content/270/1/414.short
(21) Emery, M. G.; Fisher, J. M.; Chien, J. Y.; Kharasch, E. D.; Dellinger, E. P.; Kowdley, K. V.; Thummel, K. E. CYP2E1 activity before and after weight loss in morbidly obese subjects with nonalcoholic fatty liver disease. *Hepatology* **2003**, *38* (2), 428−435.
(22) Kim, J.-H.; Cheong, H. S.; Park, B. L.; Kim, L. H.; Shin, H. J.; Na, H. S.; Chung, M. W.; Shin, H. D. Direct sequencing and comprehensive screening of genetic polymorphisms on CYP2 family genes (CYP2A6, CYP2B6, CYP2C8, and CYP2E1) in five ethnic populations. *Arch. Pharm. Res.* **2015**, *38* (1), 115−128.
(23) Yang, J.; He, M. M.; Niu, W.; Wrighton, S. A.; Li, L.; Liu, Y.; Li, C. Metabolic capabilities of cytochrome P450 enzymes in Chinese liver microsomes compared with those in Caucasian liver microsomes. *Br. J. Clin. Pharmacol.* **2012**, *73* (2), 268−284.
(24) Yang, M.; Tsuang, J.; Yvonne Wan, Y.-J. A haplotype analysis of CYP2E1 polymorphisms in relation to alcoholic phenotypes in Mexican Americans. *Alcohol.: Clin. Exp. Res.* **2007**, *31* (12), 1991−2000.
(25) Jia, W.-H.; Pan, Q.-H.; Qin, H.-D.; Xu, Y.-F.; Shen, G.-P.; Chen, L.; Chen, L.-Z.; Feng, Q.-S.; Hong, M.-H.; Zeng, Y.-X.; Shugart, Y. Y. A case-control and a family-based association study revealing an association between CYP2E1 polymorphisms and nasopharyngeal carcinoma risk in Cantonese. *Carcinogenesis* **2009**, *30* (12), 2031−2036.
(26) Nedelcheva, V.; Gut, I.; Soucek, P.; Tichavská, B.; Týnkova, L.; Mráz, J.; Guengerich, L. P.; Ingelman-Sundberg, M. Metabolism of benzene in human liver microsomes: individual variations in relation to CYP2E1 expression. *Arch. Toxicol.* **1999**, *73* (1), 33−40.
(27) Yamazaki, H.; Inui, Y.; Yun, C. H.; Guengerich, F. P.; Shimada, T. Cytochrome P450 2E1 and 2A6 enzymes as major catalysts for metabolic activation of N-nitrosodialkylamines and tobacco-related nitrosamines in human liver microsomes. *Carcinogenesis* **1992**, *13* (10), 1789−1794.
(28) Heit, C.; Dong, H.; Chen, Y.; Thompson, D. C.; Deitrich, R. A.; Vasiliou, V. K. The Role of CYP2E1 in Alcohol Metabolism and Sensitivity in the Central Nervous System. In *A. Dey (Hg.): Cytochrome P450 2E1. Its role in disease and drug metabolism, Bd. 67*; Unter Mitarbeit von Springer Verlag: Dordrecht, Netherlands, 2013; pp 235−247.
(29) Lieber, C. S. Cytochrome P-4502E1: its physiological and pathological role. *Physiol. Rev.* **1997**, *77* (2), 517−544.
(30) Gates, L. A.; Lu, D.; Peterson, L. A. Trapping of cis-2-butene-1,4-dial to measure furan metabolism in human liver microsomes by cytochrome P450 enzymes. *Drug Metab. Dispos.* **2012**, *40* (3), 596−601.
(31) Gates, L. A.; Phillips, M. B.; Matter, B. A.; Peterson, L. A. Comparative metabolism of furan in rodent and human cryopreserved hepatocytes. *Drug Metab. Dispos.* **2014**, *42* (7), 1132−1136.
(32) Peterson, L. A.; Cummings, M. E.; Vu, C. C.; Matter, B. A. Glutathione trapping to measure microsomal oxidation of furan to cis-2-butene-1,4-dial. *Drug Metab. Dispos.* **2005**, *33* (10), 1453−1458.
(33) Parmar, D.; Burka, L. T. Studies on the interaction of furan with hepatic cytochrome P-450. *J. Biochem. Toxicol.* **1993**, *8* (1), 1−9.
(34) Watzek, N.; Scherbl, D.; Feld, J.; Berger, F.; Doroshyenko, O.; Fuhr, U.; Tomalik-Scharte, D.; Baum, M.; Eisenbrand, G.; Richling, E. Profiling of mercapturic acids of acrolein and acrylamide in human urine after consumption of potato crisps. *Mol. Nutr. Food Res.* **2012**, *56* (12), 1825−1837.
(35) Stegmüller, S.; Beißmann, N.; Kremer, J. I.; Mehl, D.; Baumann, C.; Richling, E. A New UPLC-qTOF Approach for Elucidating Furan and 2-Methylfuran Metabolites in Human Urine Samples after Coffee Consumption. *Molecules* **2020**, *25* (21), 5104.
(36) Kremer, J. I.; Karlstetter, D.; Kirsch, V.; Bohlen, D.; Klier, C.; Rotermund, J.; Thomas, H.; Lang, L.; Becker, H.; Bakuradze, T.; Stegmueller, S.; Richling, E. Urinary excretion of furan and 2-methylfuran metabolites in humans after coffee consumption: a pilot study. *Metabolites* **2023**, *13* (9), 1011.
(37) Bohlen, D.; Karlstetter, D.; Leidner, J.; Kremer, J.; Kirsch, V.; Eisenbrand, G.; Bakuradze, T.; Stegmüller, S.; Richling, E. Dosimetry of human exposure to furan and 2-methylfuran by monitoring urinary biomarkers. *Food Chem. Toxicol.* **2024**, *189*, 114774.
(38) Li, W.; Hu, Z.; Sun, C.; Wang, Y.; Li, W.; Peng, Y.; Zheng, J. A Metabolic Activation-Based Chemoproteomic Platform to Profile Adducted Proteins Derived from Furan-Containing Compounds. *ACS Chem. Biol.* **2022**, *17* (4), 873−882.
(39) Adams, A.; Bouckaert, C.; van Lancker, F.; De Meulenaer, B.; De Kimpe, N. Amino acid catalysis of 2-alkylfuran formation from lipid oxidation-derived α,β-unsaturated aldehydes. *J. Sci. Food Agric.* **2011**, *59* (20), 11058−11062.
(40) Kawai, Y.; Nuka, E. Abundance of DNA adducts of 4-oxo-2-alkenals, lipid peroxidation-derived highly reactive genotoxins. *J. Clin. Biochem. Nutr.* **2018**, *62* (1), 3−10.
(41) Rentel, C.; Wang, X.; Batt, M.; Kurata, C.; Oliver, J.; Gaus, H.; Krotz, A. H.; McArdle, J. V.; Capaldi, D. C. Formation of modified cytosine residues in the presence of depurinated DNA. *J. Org. Chem.* **2005**, *70* (20), 7841−7845.
(42) Elmore, J. S.; Mottram, D. S.; Enser, M.; Wood, J. D. Effect of the polyunsaturated fatty acid composition of beef muscle on the profile of aroma volatiles. *J. Agric. Food Chem.* **1999**, *47* (4), 1619−1625.

https://doi.org/10.1021/acs.chemrestox.4c00083
Chem. Res. Toxicol. XXXX, XXX, XXX−XXX